PHYSICAL REVIEW B VOLUME 2, NUMBER 6 15 SEPTEMBER 1970

Energy-Band Structure of BeS, BeSe, and BeTe

D. J. Stukel
Aerospace Research Laboratories, Wright-Patterson Air Force Base, Ohio 45433
(Received 6 February 1970)

A first-principles self-consistent orthogonalized-plane-wave energy-band calculation has been performed for cubic BeS, BeSe, and BeTe using a nonrelativistic formalism and Slater's free-electron-exchange approximation. These are the first energy-band solutions reported for these compounds. No experimental data are available concerning the energy bands or optical properties of these semiconducting compounds. The imaginary part of the dielectric constants, spin-orbit splittings, effective masses, and x-ray form factors (Fourier transforms of the electron charge density) have been calculated.

I. INTRODUCTION

The beryllium compounds (BeS, BeSe, and BeTe) are II-VI compounds which form in the zinc-blende (cubic) structure. These compounds have not been studied experimentally except for the work of Zachariasen[1] on BeS, BeSe, and BeTe and Staritzky[2] on BeS. Zachariasen demonstrated that these compounds crystallize in the zinc-blende structure and measured their lattice constants. Staritzky confirmed Zachariasen's work on BeS. The very high toxic hazard ratings of the beryllium compounds is the primary reason for the lack of research on these compounds.

The purpose of this paper is to report for BeS, BeSe, and BeTe a theoretical calculation of the band structure, the imaginary part of the dielectric constant (ϵ_2) derived from the theoretical bands, spin-orbit splittings, effective masses, and the form factors (the Fourier transforms of the electron charge density). This is the first work, either experimental or theoretical, reported on the band structure and optical properties of these compounds.

In the past few years, a great deal of success has been attained in calculating the energy-band structures of III-V, II-VI, and IV compounds using an unadjusted first-principles self-consistent orthogonalized-plane-wave (SCOPW) model developed at Aerospace Research Laboratories. The SCOPW programs used to calculate the electronic band structure have given very good one-electron band energies for tetrahedrally bonded compounds when Slater's exchange is used.[3-6]

II. CALCULATIONAL DETAILS

A. Self-Consistent OPW Model

The orthogonalized-plane-wave (OPW) method of Herring[7] is used to calculate the electron energies. In the SCOPW model,[3,4] the electronic states are divided into tightly bound core states and loosely bound valence states. The core states must have negligible overlap from atom to atom. They are calculated from a spherically symmetrized crystalline potential.

The valence states must be well described by a modified Fourier series

$$\psi_{k_0}(r) = \sum_\mu B_\mu \left[\Omega_0^{-1/2} e^{i\vec{k}_\mu \cdot \vec{r}} - \sum_a e^{i\vec{k}_\mu \cdot \vec{R}_a} \sum A^a_{c\mu}\, \psi_c(\vec{r} - \vec{R}_a)\right] ,$$

where $\vec{k}_\mu = \vec{k}_0 + \vec{K}_\mu$, $\vec{k}_0$ locates the electron within the first Brillouin zone, $\vec{K}_\mu$ is a reciprocal-lattice vector, R_a is an atom location, ψ_c is a core wave function, and Ω_0 is the volume of the crystalline unit cell. The coefficients $A^a_{c\mu}$ are determined by requiring that $\psi_{k_0}(r)$ be orthogonal to all core-state wave functions. The variation of B_μ to minimize the energy then results in the valence one-electron energies and wave functions.

The dual requirements of no appreciable core overlap and the convergence of the valence wave-function expansion with a reasonable number of OPW's determine the division of the electron states into core and valence states. For Be, the 1s state (for S the 3s and 3p states, for Se the 4s and 4p states, and for Te the 5s and 5p states) are taken as the valence states. OPW series convergence is discussed in Sec. II B.

The calculation is self-consistent in the sense that the core and valence wave functions are calculated alternately until neither changes appreciably. The Coulomb potential due to the valence electrons and the valence charge density are both spherically symmetrized about each inequivalent atom site. With these valence quantities frozen, new core wave functions are calculated and iterated until the core wave functions are mutually self-consistent. The total electronic charge density is calculated at 650 crystalline mesh points covering $\frac{1}{24}$ of the unit cell, and the Fourier transform

of $\rho(r)^{1/3}$ is calculated. The new crystal potential is calculated from the old valence charge distribution and the new core-charge distribution. Then new core-valence orthogonality coefficients $A^a_{c\mu}$ are calculated. The iteration cycle is then completed by the calculation of new valence energies and wave functions. The iteration process is continued until the valence one-electron energies change less than 0.01 eV from iteration to iteration.

The appropriate charge density to use for both the self-consistent potential calculation and the form-factor calculation is the average charge density of all the electrons in the Brillouin zone. In the present self-consistent calculations, this average is approximated by a weighted average over electrons at the Γ, X, L, and W high-symmetry points of the Brillouin zone shown in Fig. 1. The weights are taken to be proportional to the volumes within the first Brillouin zone closest to each high-symmetry point. The adequacy of this approximation has been tested and the error in the energy eigenvalues has been shown to be less than 0.1 eV.[5]

The present self-consistent model approximates the complicated Hartree-Fock exchange potential by a term proportional to the electron charge density to the $\frac{1}{3}$ power. The best-known exchange potentials are Slater's[8] (S),

$$V_{X\,S} = -6[(3/8\pi)\,\rho(r)]^{1/3}$$

and those of Kohn and Sham[9] and Gaspar's[10] (KSG),

$$V_{X\,KSG} = -4[(3/8\pi)\,\rho(r)]^{1/3} \quad .$$

We have tried different constants of proportionality. When calculating the energy-band structure of tetrahedrally bonded semiconductors with our SCOPW model, we have found that the S exchange always gives results that agree most closely with experiment. The many-body work of Hedin, S. Lundqvist, B. Lundqvist, and co-workers supports the choice of a constant factor multiplying the exchange term.[11] To give a feeling for which transitions are most sensitive to the value of the exchange constant, both S and KSG energies will be given for selected high-symmetry point values.

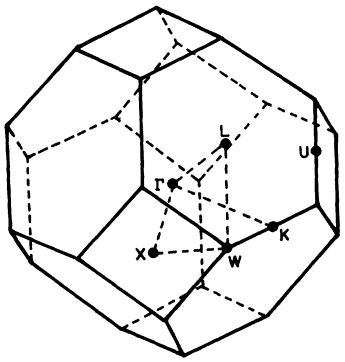

FIG. 1. Zinc-blende Brillouin zone with high-symmetry points labeled.

In order to calculate the absorptive part of the dielectric constant ϵ_2, a pseudopotential fit is made to the relevant energy levels at the Γ, X, L, and W points. The pseudopotential technique is then used to calculate energy differences and transition matrix elements throughout the Brillouin zone.[12] In our experience, this procedure gives the ϵ_2 peaks at the correct energies. However, the relative peak heights do not match experiment because of their dependence upon the poor pseudopotential wave functions, and because of complicated electron-hole and electron-phonon interactions which are ignored in our model.

One way of taking relativistic effects into account within the framework of nonrelativistic band calculations is with first-order perturbation theory. The perturbing Hamiltonian obtained for the spin-orbit splitting is

$$\hat{H}_{so} = -\tfrac{1}{4}iq^2\hat{\sigma}\cdot[\nabla V(r)\times\nabla] \quad ,$$

where $V(r)$ is the potential, $\hat{\sigma}$ is the Pauli spin operator, and q is the fine-structure constant. The Γ_{15v} SCOPW valence wave functions are used in this calculation.

B. OPW Series Convergence

A major problem involved in an OPW calculation of these beryllium compounds is the slow convergence of the OPW series expansion of the valence and conduction wave functions. In the OPW expansion, all k vectors are used whose magnitudes are smaller than some value k_{max}. The minimum distance that can be defined by the plane-wave terms in the OPW series is roughly

$$d_{min} \approx \tfrac{1}{2}\lambda_{min} = \pi/\kappa_{max} = a/2(m^2+n^2+l^2)^{1/2} \quad ,$$

where a is the lattice constant and (m,n,l) are integers defining the largest k vector. The dependence of the BeS, BeSe, and BeTe valence- and conduction-band energies upon d_{min} are shown for an OPW model in Figs. 2–4. For the convergence study, Herman's overlapping-free-atomic-potential (OAP) model[13] is used in which the potential is calculated from free-atom charge densities which are packed in the crystal lattice. It has been shown that the convergence of the SCOPW model is similar to that of Herman's OAP model.[14] The cation (Be) and anion (S, Se, and Te) core-charge densities $[4\pi r^2\rho(r)]$ are also shown in the figures.

It has been shown, using this OPW model, that the series convergence depends upon two factors.[14]

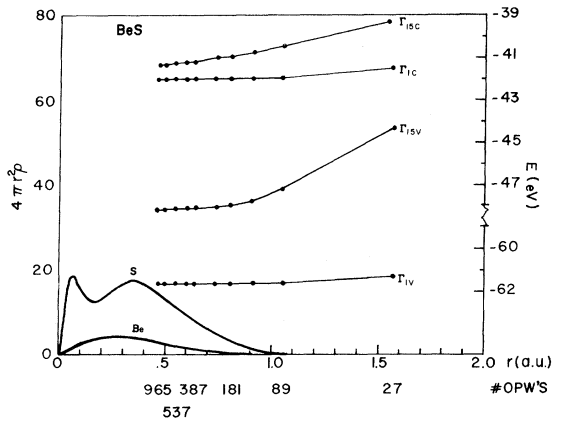

FIG. 2. Convergence study of non-self-consistent energy levels at Γ point for BeS.

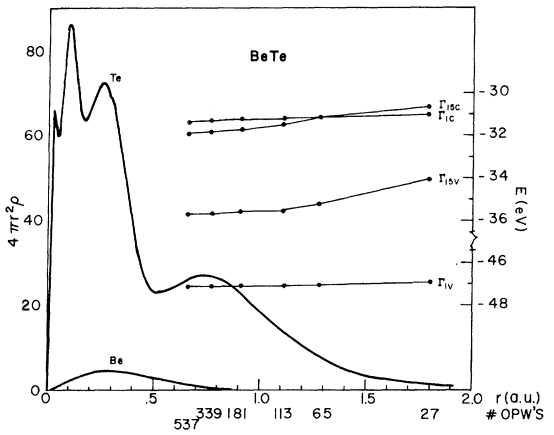

FIG. 4. Convergence study of non-self-consistent energy levels at Γ point for BeTe.

One is the relative core size of anion and cation. $d_{\min}$ depends upon the lattice constant which depends upon the sum of anion and cation core sizes. The penetration into the smaller core is thus least when the core-size ratio is most extreme. It is clear from the figures that these beryllium compounds have a fairly extreme core-size ratio (especially in the case of BeTe), and thus a relatively poor penetration into the Be core. The second factor involves the presence or absence of core wave functions in the symmetrized OPW's. If no core wave functions are present in an OPW expansion, it becomes a pure plane-wave expansion (Fourier series), with consequently poorer convergence. Be has no p states in the core, and thus the Γ_{15v} wave function contains no Be core states to aid convergence. The only saving factor is that Γ_{15v} convergence depends much more critically upon penetration into the anion than upon cation penetration. It can be seen from the figures that

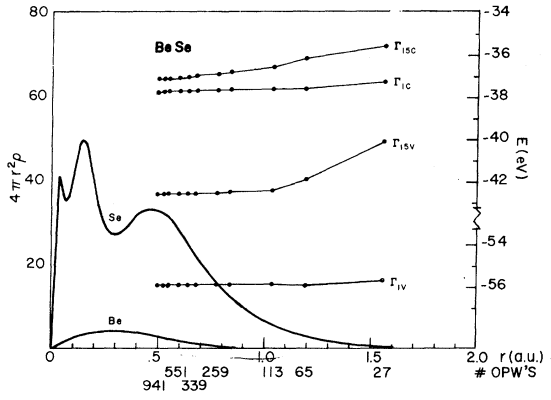

FIG. 3. Convergence study of non-self-consistent energy levels at Γ point for BeSe.

convergence of the energies is reasonably good by 459 OPW's. We estimate a maximum uncertainty of 0.3 eV in our SCOPW results due to lack of OPW convergence.

III. RESULTS

In the SCOPW[1] model, the input data consist of the crystal symmetry, the nuclear charge of the cation and anion, the lattice constant, and the exchange constant. The lattice constants used in these calculations are given in Table I.

The energy bands for the three compounds based on the S exchange and 459 OPW's at Γ (and a comparable number of OPW's at X, L, and W) are given in Figs. 5–7. The energy eigenvalues are given in Table II for BeS, BeSe, and BeTe using Slater's exchange and for BeS using the Kohn-Sham exchange. The Kohn-Sham results are only shown to indicate the effect of changing the exchange constant.

These compounds all have indirect gaps. The minimum in the conduction band occurs at X or along the Γ-X line near the X point. The next lowest conduction-band minimum occurs at the L point in these compounds. The third minimum in the conduction band occurs at the Γ point. The Γ and L point minimums are close to each other in energy but much higher than the minimum which occurs along the Γ-X line. The indirect gaps are

TABLE I. Lattice constants used in SCOPW band calculations. The lattice constants are given in Å.

Crystal	Lattice constant
BeS	4.8624 (Ref. 2)
BeSe	5.139 (Ref. 1)
BeTe	5.626 (Ref. 1)

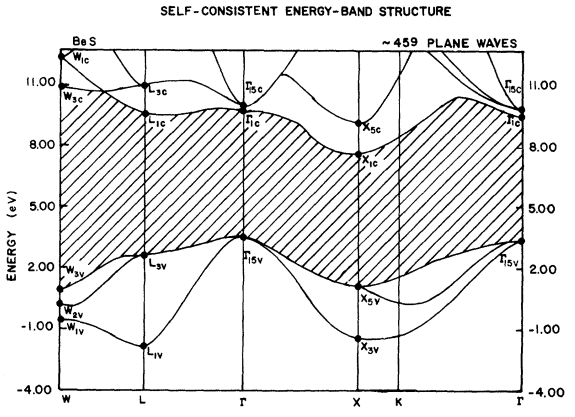

FIG. 5. SCOPW energy-band structure of BeS. The solid dots denote SCOPW energy levels. The solid lines were obtained by fitting a pseudopotential-type interpolation scheme to the SCOPW energy levels.

BeS	4.17 eV	occurs at X point
BeSe	3.61 eV	occurs at X point
BeTe	2.89 eV	occurs at 0.84 distance from Γ to X point .

The imaginary part of the dielectric constants (ϵ_2) are given in Figs. 8–10. The location of some of the major transitions are also indicated. The shape of the ϵ_2 curves are very similar to other cubic group II-VI, III-V, and IV compounds. Generally there are three peaks, the first due to transitions closely related to the L_{1c}-L_{3v} transition. This peak is usually small and obscured by the second peak which is very large. The second peak originates in the outer part of the zone (U-

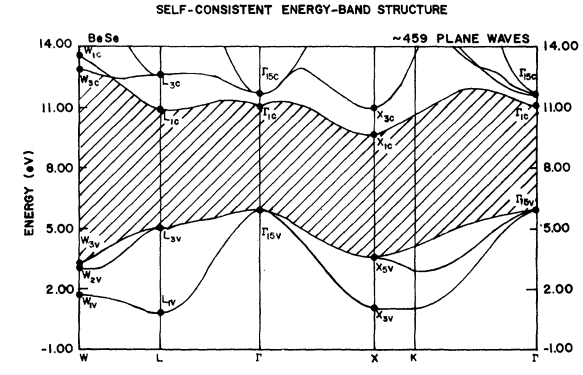

FIG. 6. SCOPW energy-band structure of BeSe. The solid dots denote SCOPW energy levels. The solid lines were obtained by fitting a pseudopotential-type interpolation scheme to the SCOPW energy levels.

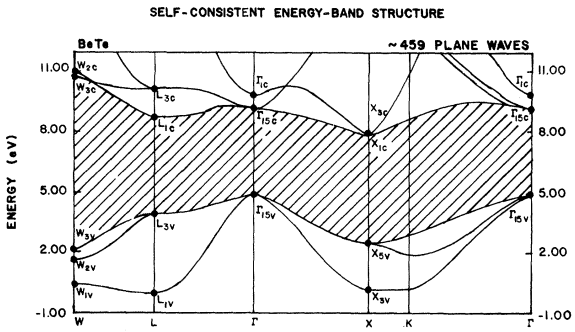

FIG. 7. SCOPW energy-band structure of BeTe. The solid dots denote SCOPW energy levels. The solid lines were obtained by fitting a pseudopotential-type interpolation scheme to the SCOPW energy levels.

K) region and is usually straddled by the X_{1c}-X_{5v} and X_{3c}-X_{5v} transitions. The third peak is due to transition closely related to the L_{3c}-L_{3v} transition.

Effective masses have been calculated for the

TABLE II. Self-consistent energy eigenvalues for cubic BeS, BeSe, and BeTe based on Slater's and Kohn and Sham's exchange and a four-point (Γ, X, L, and W) zone sampling. 459 OPW's were used at Γ and a comparable number of OPW's at X, L, and W. The zero of energy has been placed at the top of the valence band (Γ_{15v}). All entries are in eV.

	BeS		BeSe	BeTe
Level	Slater	Kohn and Sham	Slater	Slater
Γ_{15c}	6.50	5.43	5.61	4.19
Γ_{1c}	6.14	5.52	5.02	4.89
Γ_{15v}	0.0	0.0	0.0	0.0
Γ_{1v}	−13.33	−13.54	−13.36	−11.46
X_{3c}	5.76	4.57	4.80	3.17
X_{1c}	4.17	2.60	3.61	2.94
X_{5v}	−2.33	−2.75	−2.37	−2.35
X_{3v}	−4.59	−5.18	−4.71	−4.75
X_{1v}	−11.41	−11.25	−11.66	−9.59
X_{1c}-X_{5v}	6.50	5.35	5.98	5.29
X_{3c}-X_{5v}	8.09	7.32	7.17	5.52
L_{3c}	7.45	6.27	6.63	5.18
L_{1c}	5.99	5.20	4.88	3.77
L_{3v}	−0.91	−1.07	−0.96	−0.99
L_{1v}	−5.22	−6.01	−5.22	−5.08
L_{1v}	−11.89	−16.82	−12.09	−10.10
L_{3c}-L_{3v}	8.36	7.34	7.59	6.17
L_{1c}-L_{3v}	6.90	6.27	5.84	4.76
W_{2c}	9.09	7.74	8.12	6.21
W_{3c}	7.20	6.05	6.81	5.87
W_{3v}	−2.87	−3.54	−2.88	−2.81
W_{2v}	−3.39	−4.06	−3.39	−3.30
W_{1v}	−3.93	−4.35	−4.12	−4.27
W_{4v}	−11.38	−11.18	−11.63	−9.56
W_{3c}-W_{3v}	10.07	9.59	9.69	8.68

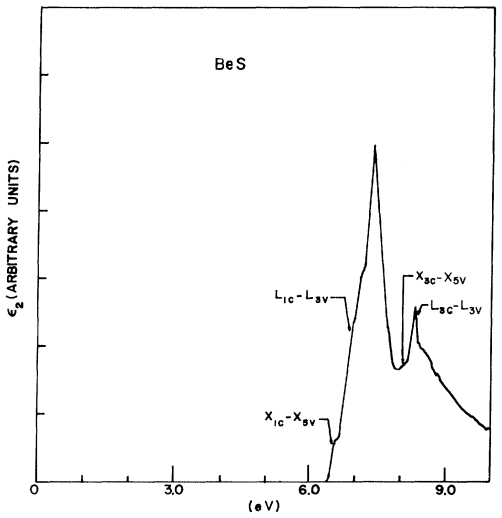

FIG. 8. Theoretical ϵ_2 curve for BeS with the location of the high-symmetry point transition shown.

top valence band (where spin-orbit splitting has been neglected) at the Γ point for both the heavy and light hole in the [1, 0, 0] and [1, 1, 1] direction. The electron effective mass at the minimum in the conduction band has been calculated in the [1, 0, 0] direction. These effective masses are presented in Table III.

The spin-orbit splitting at $k = 0$ of the top Γ_{15v} valence band into Γ_7 and Γ_8 bands has been found by use of first-order perturbation theory on the self-consistent Slater Γ_{15v} wave functions. The calculated values are presented in Table IV.

In Table V, theoretical Fourier components of the charge density (the x-ray form factors) are

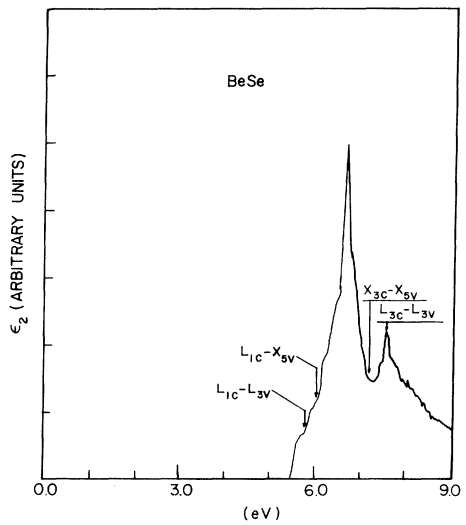

FIG. 9. Theoretical ϵ_2 curve for BeSe with the location of the high-symmetry point transition shown.

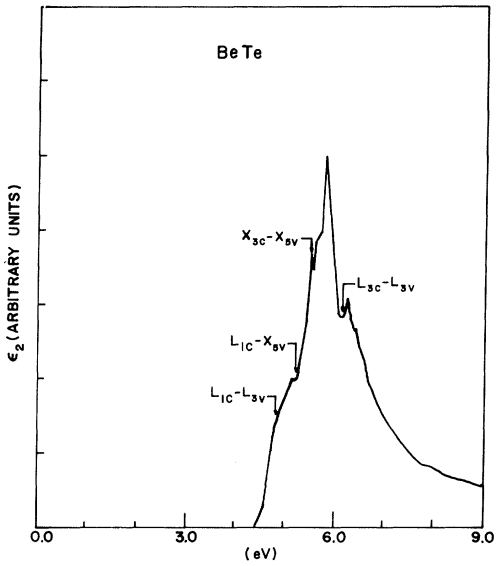

FIG. 10. Theoretical ϵ_2 curve for BeTe with the location of the high-symmetry point transition shown.

given. The Fourier components in the column headed RHF are obtained by the superposition of relativistic Hartree-Fock free atoms placed in the crystalline lattice. The columns are headed with the exchange potential used in the SCOPW model. From the BeS form factors in Table III, it can be seen that for the high reflections, the RHF results agree with the results obtained using Kohn and Sham's exchange potential. This good agreement illustrates the well-known result that the Kohn-Sham wave functions are very good for free-atom calculations. It has been found that for the low reflections, the RHF results are generally too small in semiconductors. The opposite result applies in metals where the valence charge spreads out. It has been found that Slater results generally give slightly better agreement with experiment for lower reflections.[15]

TABLE III. Effective masses for the top of the valence band (where spin-orbit splitting has been neglected) at the Γ point [calculated in the [1, 0, 0] and the [1, 1, 1] directions] and for the bottom conduction band at the Γ-X minimum (calculated in the [1, 0, 0] direction).

	m_v^* at Γ in [1, 0, 0] direction		m_v^* at Γ in [1, 1, 1] direction		m_v^* at Γ-X minimum in [1, 0, 0] direction
	Heavy hole	Light hole	Heavy hole	Light hole	
BeS	0.7	0.4	1.7	0.3	1.0
BeSe	0.6	0.3	1.3	0.2	1.2
BeTe	0.7	0.5	1.2	0.3	1.4

TABLE IV. Spin-orbit splitting of the Γ_{15v} level ($\Gamma_8 - \Gamma_7$) calculated by first-order perturbation theory using the self-consistent wave functions. All energies are in eV.

BeS	0.11
BeSe	0.57
BeTe	0.79

IV. CONCLUSIONS

These results are based almost completely on first principles with no adjustment to fit experiment. The only experimental datum used is the lattice constant. Slater's exchange approximation is made. The use of this approximation is supported by our experience on many tetrahedrally bonded semiconductors and by the many-body work of Hedin, S. Lundqvist, and B. Lundqvist. Their work indicates that Slater's approximation includes the effects of correlation. Relativity has been neglected. Changes due to relativity are expected to be insignificant for BeS (0.1 eV), small for BeSe (0.2–0.4 eV), but significant for BeTe (0.4–1.0 eV).

The validity of the theoretical results presented in this paper depends upon the applicability of Slater's exchange approximation, the validity of the SCOPW model, the size of the relativistic shifts (especially for BeTe), and the convergence of the wave-functions expansions. Past experience on many tetrahedral compounds gives us considerable faith in the validity of these results.

It is clear from this work that these compounds have tremendous potential if the toxic-hazard problem can be overcome. The need for experimental investigation on these compounds is evident.

ACKNOWLEDGMENTS

The author wishes to thank Dr. R.N. Euwema for his interest, encouragement, and support of this work. He is also grateful to G. Schantz for his drafting of the figures.

TABLE V. Theoretical BeS, BeSe, and BeTe structure factors in electron per crystallographic unit cell. The RHF values are relativistic free-atomic Hartree-Fock results. KS and S refer to the use of the Kohn-Sham-Gaspar or the Slater exchange approximation. 459 OPW's were used in the wave-function expansion.

	BeS			BeSe		BeTe	
hkl	RHF	S	KS	RHF	S	RHF	S
111	47.72	49.64	48.45	113.70	115.57	178.63	180.31
200	35.73	36.71	35.73	100.39	101.42	163.27	164.18
220	43.58	44.18	43.36	103.45	104.23	161.85	162.61
311	34.54	34.55	34.07	90.53	90.84	145.56	145.92
222	26.86	27.00	26.67	82.06	82.52	136.07	136.69
400	37.02	37.06	36.61	88.66	89.12	140.03	140.55
331	30.28	30.64	30.26	78.90	79.72	128.08	129.04
420	23.64	23.77	23.59	71.63	72.25	120.08	120.77
224	33.38	36.66	33.14	78.72	79.55	125.67	126.52
115	27.51	27.73	27.34	70.38	71.15	115.74	116.44
333	27.51	27.68	27.28	70.38	71.11	115.74	116.40

[1]W. Zachariasen, Z. Physik. Chem. (Leipzig) 119, 210 (1926); 124, 277 (1926); 124, 440 (1926).

[2]E. Staritzky, Anal. Chem. 28, 915 (1956).

[3]R. N. Euwema, T. C. Collins, D. G. Shankland, and J. S. DeWitt, Phys. Rev. 162, 710 (1967)(CdS).

[4]D. J. Stukel, R. N. Euwema, T. C. Collins, F. Herman, and R. K. Kortum, Phys. Rev. 179, 740 (1969) (ZnS, ZnSe, CdS, CdSe).

[5]D. J. Stukel and R. N. Euwema, Phys. Rev. 186, 754 (1969) (AlP); 188, 1193 (1969) (AlAs); Phys. Rev. B 1, 1635 (1970) (Si); D. J. Stukel, T. C. Collins, and R. N. Euwema (unpublished) (GaP); D. J. Stukel, Phys. Rev. B 1, 4791 (1970) (BAs); 1, 3458 (1970) (BP); D. J. Stukel and R. N. Euwema (unpublished) (InAs, InP); T. C. Collins, D. J. Stukel, and R. N. Euwema, Phys. Rev. B 1, 724 (1970) (GaAs); R. N. Euwema and D. J. Stukel (unpublished) (SiC).

[6]D. J. Stukel, R. N. Euwema, T. C. Collins, and V. Smith, Phys. Rev. B 1, 779 (1970).

[7]C. Herring, Phys. Rev. 57, 1169 (1940).

[8]J. C. Slater, Phys. Rev. 81, 385 (1951).

[9]W. Kohn and L. J. Sham, Phys. Rev. 140, A1133 (1965).

[10]R. Gaspar, Acta Phys. Acad. Sci. Hung. 3, 263 (1954).

[11]For a review of this work the reader can refer to the excellent review article by L. Hedin and S. Lundqvist, in *Solid State Physics*, edited by F. Seitz and D. Turnbull (Academic, New York, to be published).

[12]R. N. Euwema, D. J. Stukel, T. C. Collins, J. S. DeWitt, and D. G. Shankland, Phys. Rev. 178, 1419 (1969).

[13]F. Herman and S. Skillman, in *Proceedings of the International Conference on Semiconductor Physics, Prague*, 1960 (Publishing House of Czechoslovak Academy of Science, Prague, 1961), p. 20.

[14]R. N. Euwema and D. J. Stukel, Phys. Rev. B 1, 4692 (1970).

[15]P. M. Raccah, R. N. Euwema, D. J. Stukel, and T. C. Collins, Phys. Rev. B 1, 756 (1970).

PHYSICAL REVIEW B VOLUME 2, NUMBER 6 15 SEPTEMBER 1970

Spontaneous-Raman-Scattering Efficiency and Stimulated Scattering in Silicon†

J. M. Ralston and R. K. Chang*
Dunham Laboratory, Yale University, New Haven, Connecticut 06520
(Received 5 March 1970)

The absolute spontaneous-Raman-scattering efficiency and linewidth of the 521-cm^{-1} optical mode of silicon have been measured at 77 K using a continuous laser (Nd in yttrium aluminum garnet) operating at 1.064 μm. The measured scattering efficiency (5.1×10^{-6}/cm sr for unpolarized forward scattering along the crystal [111] direction) and narrow linewidth yield a calculated value of the stimulated Raman gain coefficient which is considerably larger than those reported for other media, both solid and liquid. Stimulated Raman scattering in Si at 77 K has also been observed using a focused multimode Q-switched YAG: Nd laser. Inaccuracy in the measured stimulated gain resulted mainly from the uncertainty in the effective focal volume inside the silicon. Multiphoton absorption at the incident laser frequency has been considered and found to modify the measured stimulated gain by a significant amount. The estimated gain from the stimulated Raman effect was found to be in satisfactory agreement with that calculated from the absolute spontaneous-Raman-scattering efficiency.

I. INTRODUCTION

The near equality of the 1.064-μm laser photon energy (1.165 eV) to the indirect energy gap ($\Gamma'_{25}\rightarrow\Delta_1$) of silicon (1.17 eV at 0 K) suggests the possibility of resonant enhancement of the Raman scattering from the 521-cm^{-1} optic mode when the sample is cooled to 77 K and below. Previous investigators, using laser radiation to which silicon is opaque, have obtained values for the Raman-scattering efficiency of silicon relative to other media. Russell,[1] using reflection techniques and a 0.6328-μm laser, obtained a ratio of 35 for the scattering efficiency of silicon relative to diamond, but did not analyze his results in terms of crystal orientation and laser polarization. Parker *et al.*[2] have reported measurements of silicon's scattering intensity relative to that of germanium, using a 0.488-μm laser to which both crystals are opaque. Using general estimates for relevant parameters such as the deformation potential, Loudon[3] has suggested the scattering efficiency of homopolar semiconductors to be 10^{-6}–10^{-7}/cm sr. Most recently, Mooradian[4] has given a value of 5×10^{-6} $cm^{-1}sr^{-1}$ for the scattering efficiency of silicon using a 1.06-μm laser (Nd in yttrium aluminum garnet), and gallium arsenide as a reference medium.

We have measured with a continuous YAG: Nd laser and with due attention to crystal orientation and polarization, the spontaneous-Raman-scattering efficiency of silicon relative to liquids whose absolute scattering cross sections are known.[5] The fact that silicon at 77 K is transparent[6] to the YAG: Nd laser ($\alpha=0.034$ cm^{-1}) and the Stokes radiation ($\alpha=0.008$ cm^{-1}) allows an accurate measurement of the scattering efficiency. That is, the uncertain effect of surface condition on Raman-scattered intensity is not as important as in the case when the crystal strongly absorbs the incident radiation. We have also observed stimulated Raman scattering using a focused multimode Q-switched YAG: Nd laser. The experimental arrangements for the spontaneous and stimulated scattering will be discussed in Sec. II. In Sec. III, the stimulated Raman gain coefficient will be calculated from the spontaneous-Raman-scattering efficiency and compared with that estimated from the stimulated-Raman-scattering data.

II. EXPERIMENT

Spontaneous Scattering

A continuous YAG: Nd laser of approximately 2-W output of unpolarized radiation is weakly focused into the silicon sample, 1.3 cm in length, cooled to 77 K in a cold-finger Dewar. The silicon, of high purity (> 10 000 Ωcm), was mounted with